

**Transformations of Silver(I) Chalcogenide Clusters Induced by
Halide Ions as Dopant Components rather than Surface Kinetics
Species**

Yu-Quan Gao, Wei-Hong Wu, Hui Mao, Ya-Ge Zhang, Cai-Hong Zhan*, Zhan-Guo Jiang*

Key Laboratory of the Ministry of Education for Advanced Catalysis Materials,
Institute of Physical Chemistry, College of Chemistry and Materials Science, Zhejiang
Normal University

E-mail: chzhan@zjnu.cn; jzg@zjnu.cn.

Experimental Section

Chemicals

All chemicals and solvents obtained from suppliers were used without further purification. All solvents were analytical grade reagent.

Characterization

UV–vis spectra were measured on an Analytik Jena S600 UV–visible spectrophotometer. PL spectra were carried out with an RF-6000 fluorescence spectrometer. X-ray photoelectron spectroscopy (XPS) survey was conducted by a VG multilab ESCA system. High resolution mass spectrometry was recorded on an Agilent 6224 (Agilent Technologies, USA) ESI-TOF-MS spectrometer.

Crystal data and structure refinement

Single-crystal X-ray diffraction data collection was recorded on Bruker D8 VENTURE diffractometer equipped with a PHOTON 100 CMOS bidimensional detector and MoK α monochromatized radiation ($\lambda = 0.71073 \text{ \AA}$). The structure was solved by intrinsic phasing methods and refined by full-matrix least squares using the SHELX-TL package and OLEX 2.

Specific Refinement Details as follow: All Ag Cl S Br and atoms and part coordinated CCBu^t ligands were located in the electron density. All heavy Ag Cl S and Br atoms were refined with anisotropic thermal parameters. DFIX restraints were applied to keep some bond lengths of Bu^t and counter ions in reasonable ranges. SIMU restraints were also used for all C and some disordered silver atoms and counter ions of SbF₆⁻. Solvent molecules were taken into account with the SQUEEZE/PLATON procedure.

In all, despite an R₁ value that was a less than ideal and resolution that was poorer than generally obtained in crystallography of some small molecules, a reasonable quality refinement was achieved, and the current data is more than adequate for establishing the average connectivity of the structure. Crystallographic data for single-crystal X-ray diffraction studies are summarized in Table S1-3. Further details about of the crystal structure determinations may be obtained free of charge at <http://www.ccdc.cam.ac.uk/>. CCDC 2278716, 2278717, 2278735.

Table 1 Crystal data and structure refinement for $\{\text{Ag}_{45}(\text{ClS})_6\}^{\text{a}}$.

Empirical formula	$\text{C}_{192}\text{H}_{288}\text{Ag}_{45}\text{Cl}_6\text{F}_{24}\text{Sb}_4$
Formula weight	8606.06
Temperature/K	150.00
Crystal system	triclinic
Space group	$P-1$
$a/\text{\AA}$	19.854(4)
$b/\text{\AA}$	20.442(4)
$c/\text{\AA}$	20.492(4)
$\alpha/^\circ$	102.885(6)
$\beta/^\circ$	116.443(5)
$\gamma/^\circ$	108.691(6)
Volume/ \AA^3	6364(2)
Z	1
$\rho_{\text{calc}}/\text{g/cm}^3$	2.245
μ/mm^{-1}	3.902
F(000)	4077.0
Crystal size/ mm^3	$0.12 \times 0.11 \times 0.1$
Radiation	MoK α ($\lambda = 0.71073$)
2Θ range for data collection/ $^\circ$	4.482 to 41.63
Index ranges	$-19 \leq h \leq 19, -20 \leq k \leq 20, -19 \leq l \leq 20$
Reflections collected	35923
Independent reflections	13225 [$R_{\text{int}} = 0.0864, R_{\text{sigma}} = 0.0995$]
Data/restraints/parameters	13225/1478/1264
Goodness-of-fit on F^2	1.352
Final R indexes [$I \geq 2\sigma(I)$]	$R_1 = 0.1303, wR_2 = 0.3589$
Final R indexes [all data]	$R_1 = 0.2004, wR_2 = 0.4174$
Largest diff. peak/hole / $e \text{\AA}^{-3}$	3.45/-2.22

a, the crystal data only contains six chlorines, but ESI, EDX and XPS data imply the multi-dispersity of Cl and S in the cluster. Due to the poor quality of the data, it was not further refined with bromine and sulfur as co-occupied.

Table 2 Crystal data and structure refinement for $\{\text{Ag}_{45}(\text{BrS})_6\}^{\text{a}}$.

Empirical formula	$\text{Ag}_{45}\text{Br}_6\text{C}_{192}\text{F}_{24}\text{Sb}_4$
Formula weight	8582.53
Temperature/K	273.15
Crystal system	triclinic
Space group	<i>P</i> -1
<i>a</i> /Å	18.711(5)
<i>b</i> /Å	20.882(6)
<i>c</i> /Å	21.381(6)
α /°	110.987(9)
β /°	114.356(9)
γ /°	99.657(9)
Volume/Å ³	6599(3)
<i>Z</i>	1
$\rho_{\text{calc}}/\text{g}/\text{cm}^3$	2.160
μ/mm^{-1}	4.609
<i>F</i> (000)	3897.0
Crystal size/ mm^3	0.13 × 0.12 × 0.11
Radiation	MoK α (λ = 0.71073)
2 θ range for data collection/°	4.424 to 31.98
Index ranges	-14 ≤ <i>h</i> ≤ 14, -16 ≤ <i>k</i> ≤ 16, -14 ≤ <i>l</i> ≤ 16
Reflections collected	19809
Independent reflections	6412 [<i>R</i> _{int} = 0.0954, <i>R</i> _{sigma} = 0.1117]
Data/restraints/parameters	6412/2681/1222
Goodness-of-fit on <i>F</i> ²	1.498
Final <i>R</i> indexes [<i>I</i> ≥ 2 σ (<i>I</i>)]	<i>R</i> ₁ = 0.1364, <i>wR</i> ₂ = 0.3699
Final <i>R</i> indexes [all data]	<i>R</i> ₁ = 0.1938, <i>wR</i> ₂ = 0.4185
Largest diff. peak/hole / e Å ⁻³	2.24/-1.15

a, the crystal data only contains six bromines, but ESI, EDX and XPS data imply the multi-dispersity of Br and S in the cluster. Due to the poor quality of the data, it was not further refined with bromine and sulfur as co-occupied.

Table 3 Crystal data and structure refinement for {Ag₁₄₈(BrS)₅₆}.

Empirical formula	C ₃₆₀ H ₅₄₀ Ag ₁₄₈ Br ₃₀ S ₂₆
Formula weight	24063.51
Temperature/K	150.0
Crystal system	tetragonal
Space group	P4/mnc
a/Å	30.517(4)
b/Å	30.517(4)
c/Å	35.190(6)
α/°	90
β/°	90
γ/°	90
Volume/Å ³	32773(11)
Z	2
ρ _{calc} /g/cm ³	2.439
μ/mm ⁻¹	6.242
F(000)	22244.0
Crystal size/mm ³	0.12 × 0.11 × 0.1
Radiation	MoKα (λ = 0.71073)
2θ range for data collection/°	1.766 to 37.694
Index ranges	-27 ≤ h ≤ 25, -27 ≤ k ≤ 27, -31 ≤ l ≤ 31
Reflections collected	58977
Independent reflections	6603 [R _{int} = 0.0919, R _{sigma} = 0.0565]
Data/restraints/parameters	6603/1148/671
Goodness-of-fit on F ²	1.511
Final R indexes [I ≥ 2σ (I)]	R ₁ = 0.1233, wR ₂ = 0.3418
Final R indexes [all data]	R ₁ = 0.1586, wR ₂ = 0.3783
Largest diff. peak/hole / e Å ⁻³	5.21 ^a /-2.02

a: the 5.21 electron density peak at the very center of the cluster may be attributed to a disordered anion.

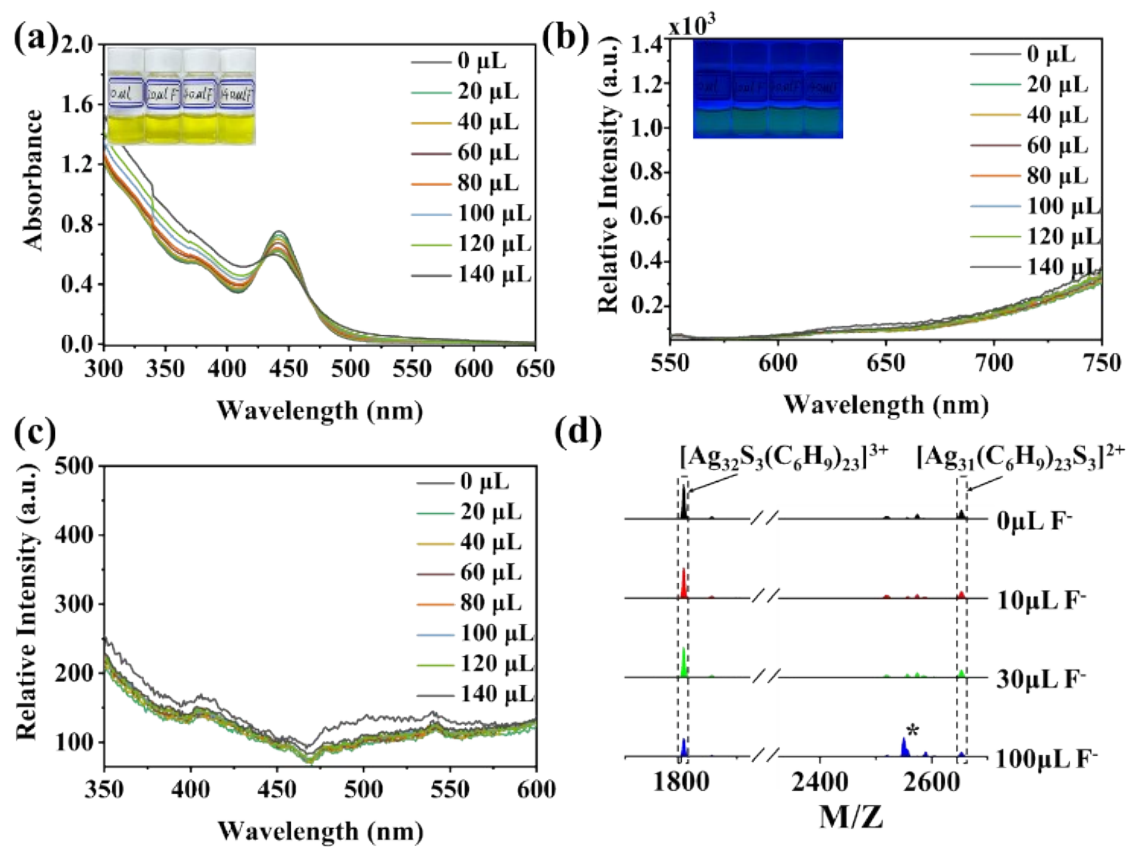


Figure S1. The UV/Vis spectra (a), emission spectra (b), excitation spectra (c), and positive-ion mode ESI-MS (d) of $\{Ag_{32}S_3\}$ at varying F^- amounts. $*[Ag_{45}S_4Cl_2]^{3+}$ was formed by trace amounts of Cl^- in solvent.

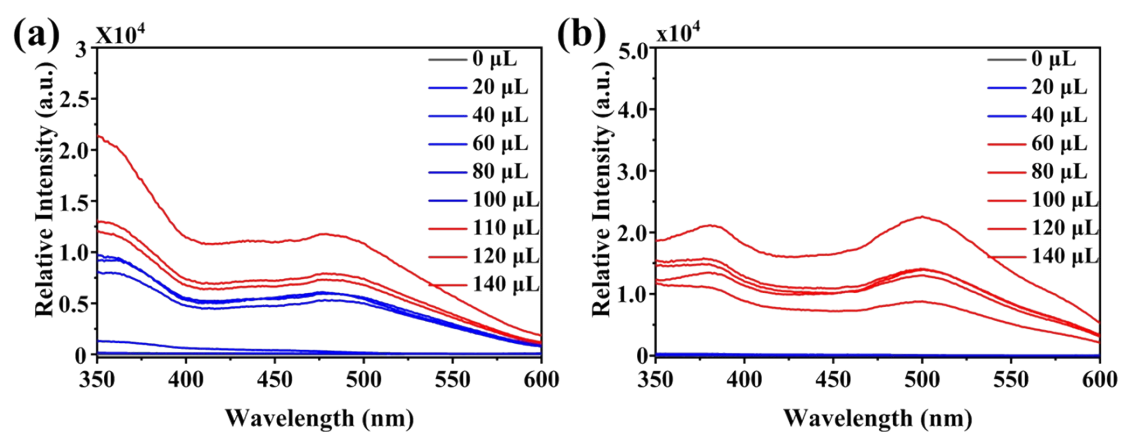


Figure S2. excitation spectra of methanolic solutions of $\{Ag_{32}S_3\}$ with different concentrations of halide ions (X^-). (a) Cl^- . (b) Br^- .

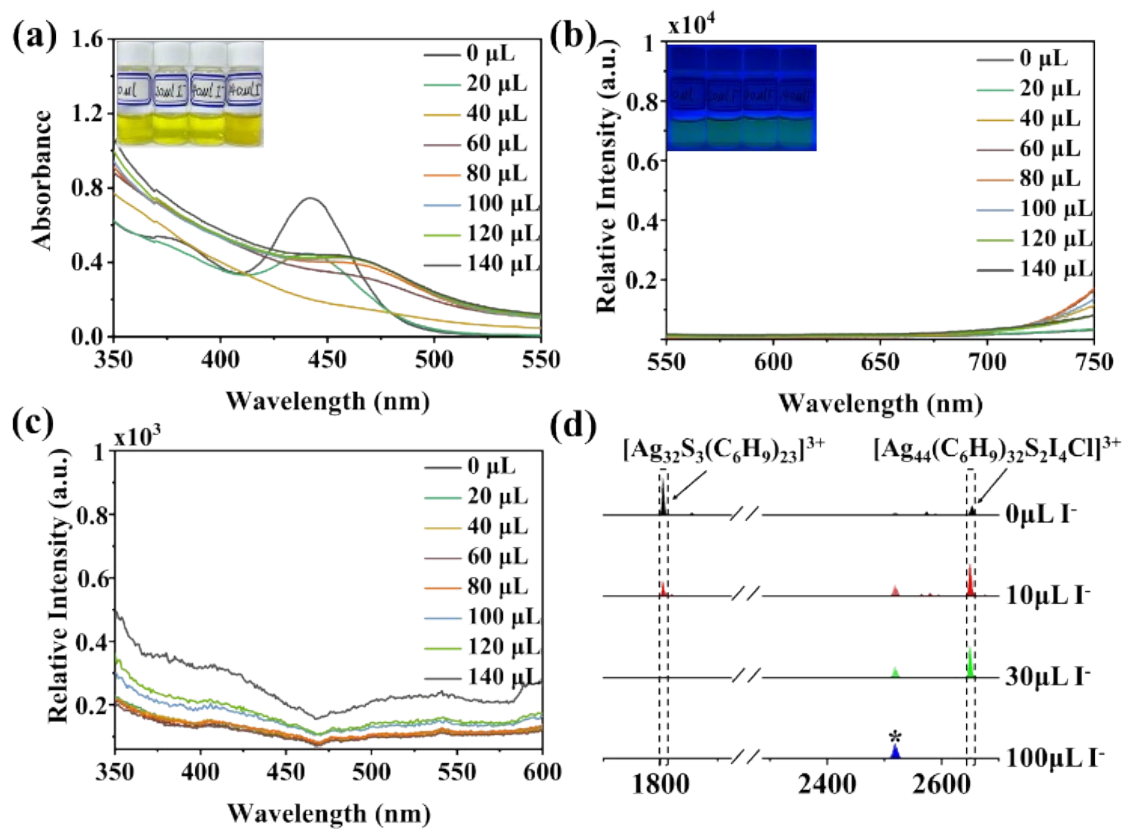


Figure S3. The UV/Vis spectra (a), emission spectra (b), excitation spectra (c), and positive-ion mode ESI-MS (d) of $\{Ag_{32}S_3\}$ at varying I^- amounts. $*[Ag_{14}(C_6H_9)_{12}Cl]^+$.



Figure S4. Pictures of solutions of $\{Ag_{32}S_3\}$ with different halogen ions added under laser pointer illumination.

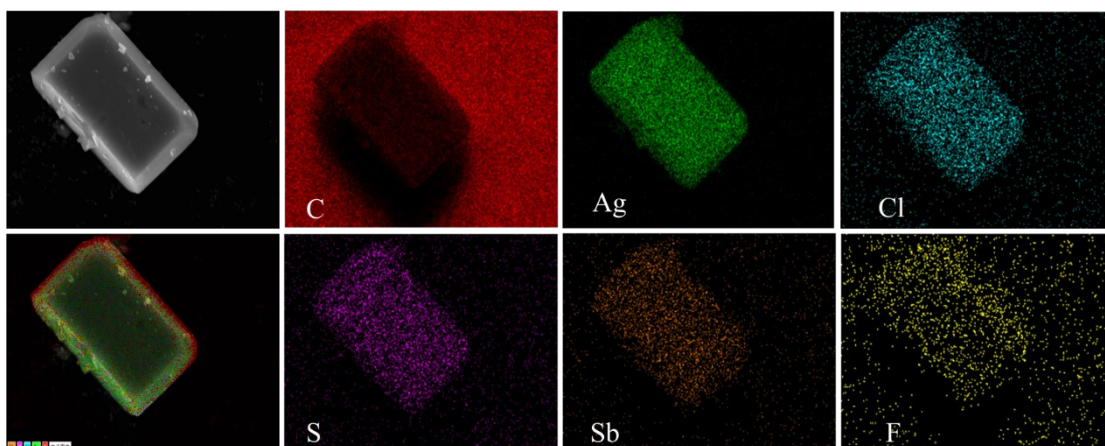


Figure S5. The energy dispersive spectroscopy (EDS) mapping results on an SEM image of single particle of $\{Ag_{45}(ClS)_6\}$. The scale bar is 5 μm .

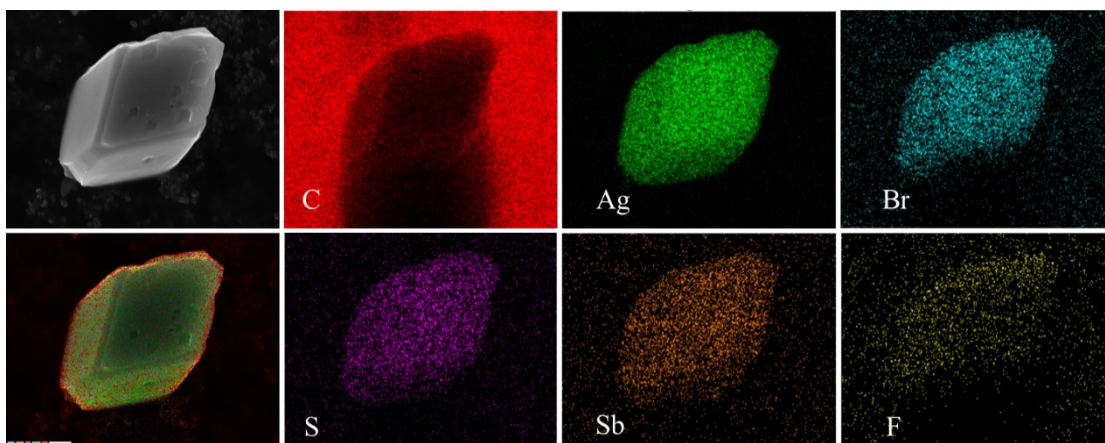


Figure S6. The energy dispersive spectroscopy (EDS) mapping results on an SEM image of single particle of $\{Ag_{45}(BrS)_6\}$. The scale bar is 2.5 μm .

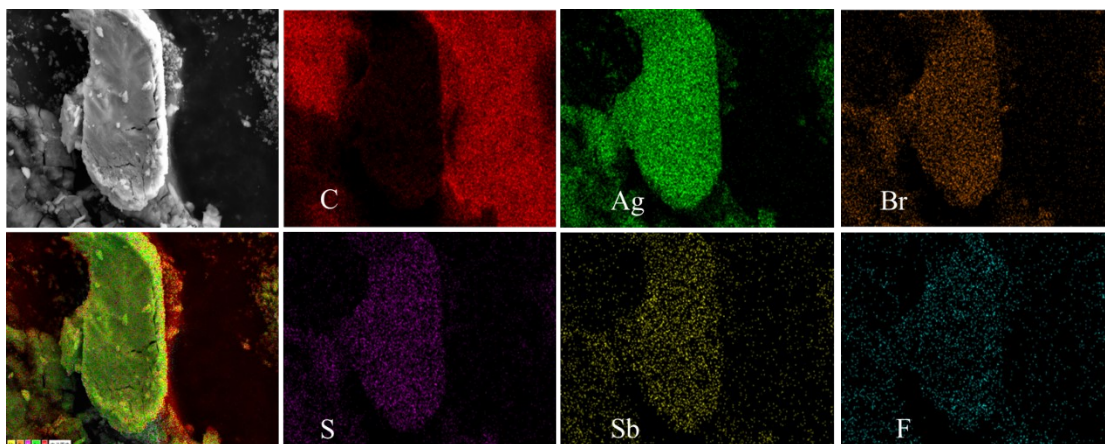


Figure S7. The energy dispersive spectroscopy (EDS) mapping results on an SEM image of single particle of $\{Ag_{148}(BrS)_{56}\}$. The scale bar is 10 μm .

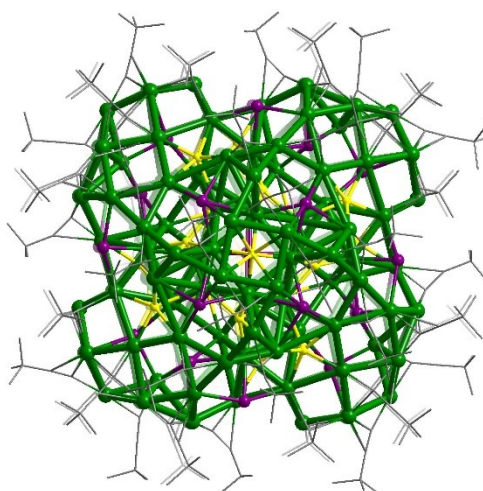
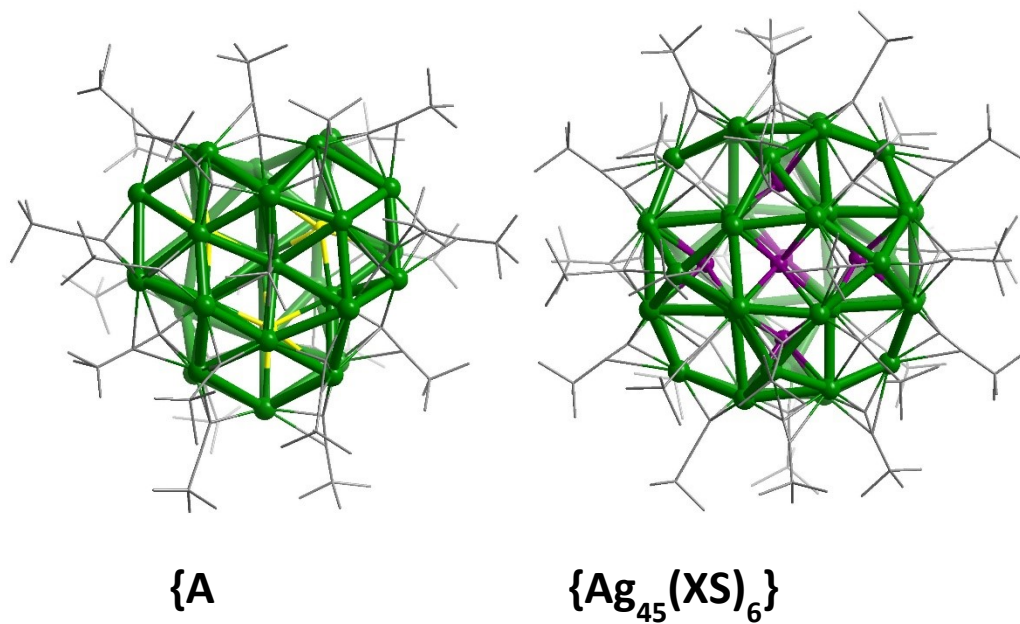


Figure S8. The structures of $\{\text{Ag}_{32}\text{S}_3\}$, $\{\text{Ag}_{45}(\text{BrS})_6\}$, $\{\text{Ag}_{148}(\text{BrS})_{56}\}$.

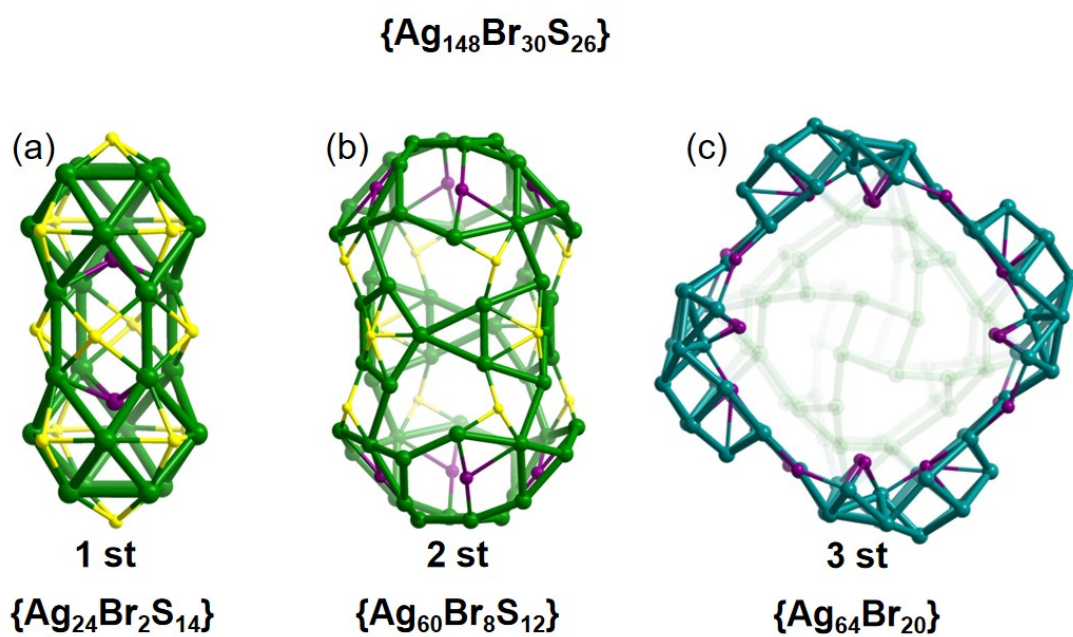


Figure S9. The positions of the Br shown in violet in the $\{\text{Ag}_{148}(\text{BrS})_{56}\}$. S and Cl in previously reported $\{\text{Ag}_{148}(\text{ClS})_{56}\}$ cannot be distinguished due to their similar electron densities.

The crystal data only contains thirty bromines, but ESI, EDX and XPS data imply the multi-dispersity of Br and S in the cluster.

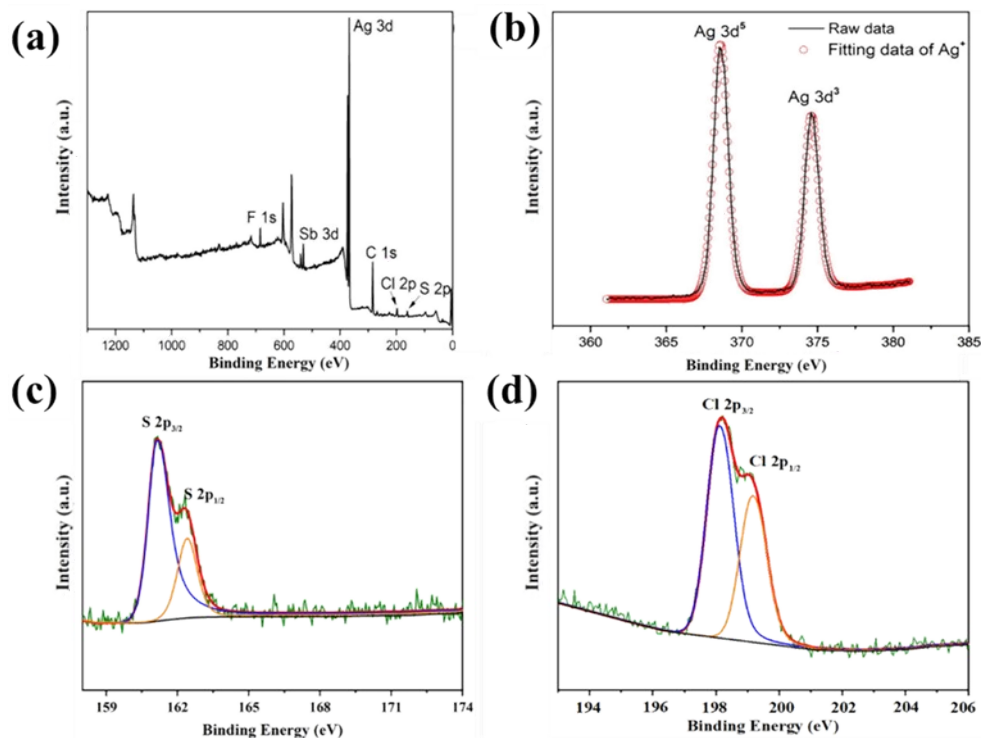


Figure S10. (a) XPS spectrum of Ag_{148}Cl ; (b), (c) and (d) are the high resolution XPS spectra of Ag, S and Cl in $\{\text{Ag}_{148}(\text{ClS})_{56}\}$, respectively.

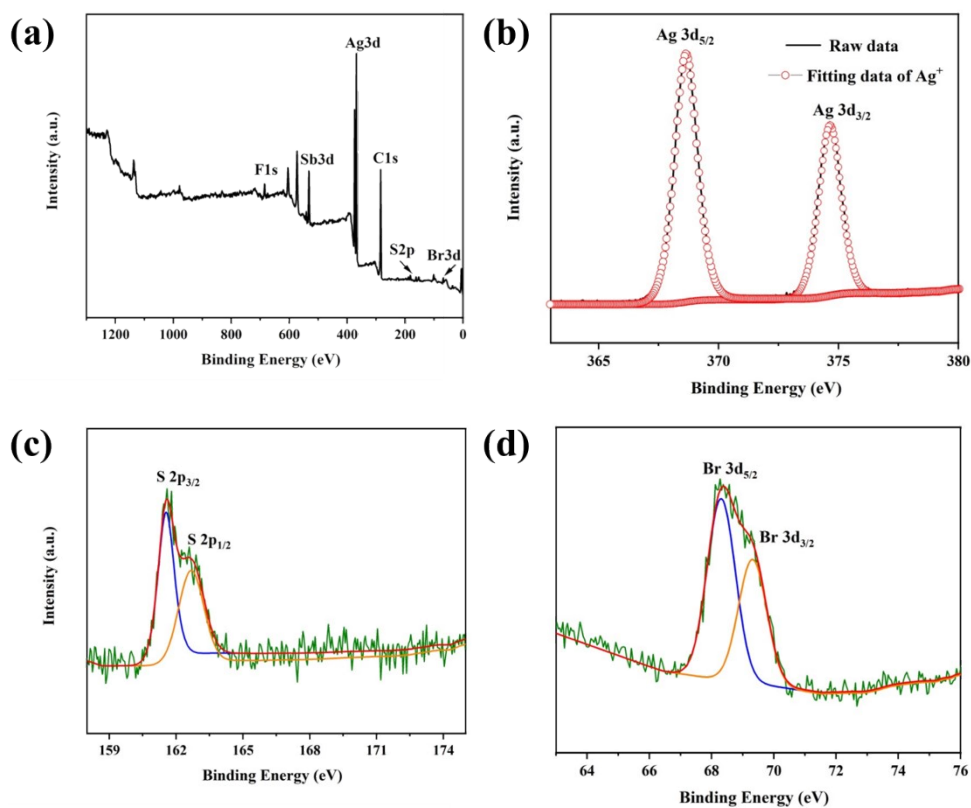


Figure S11. (a) XPS spectrum of Ag_{148}Br ; (b), (c) and (d) are the high resolution XPS spectra of Ag, S and Br in $\{\text{Ag}_{148}(\text{BrS})_{56}\}$, respectively.

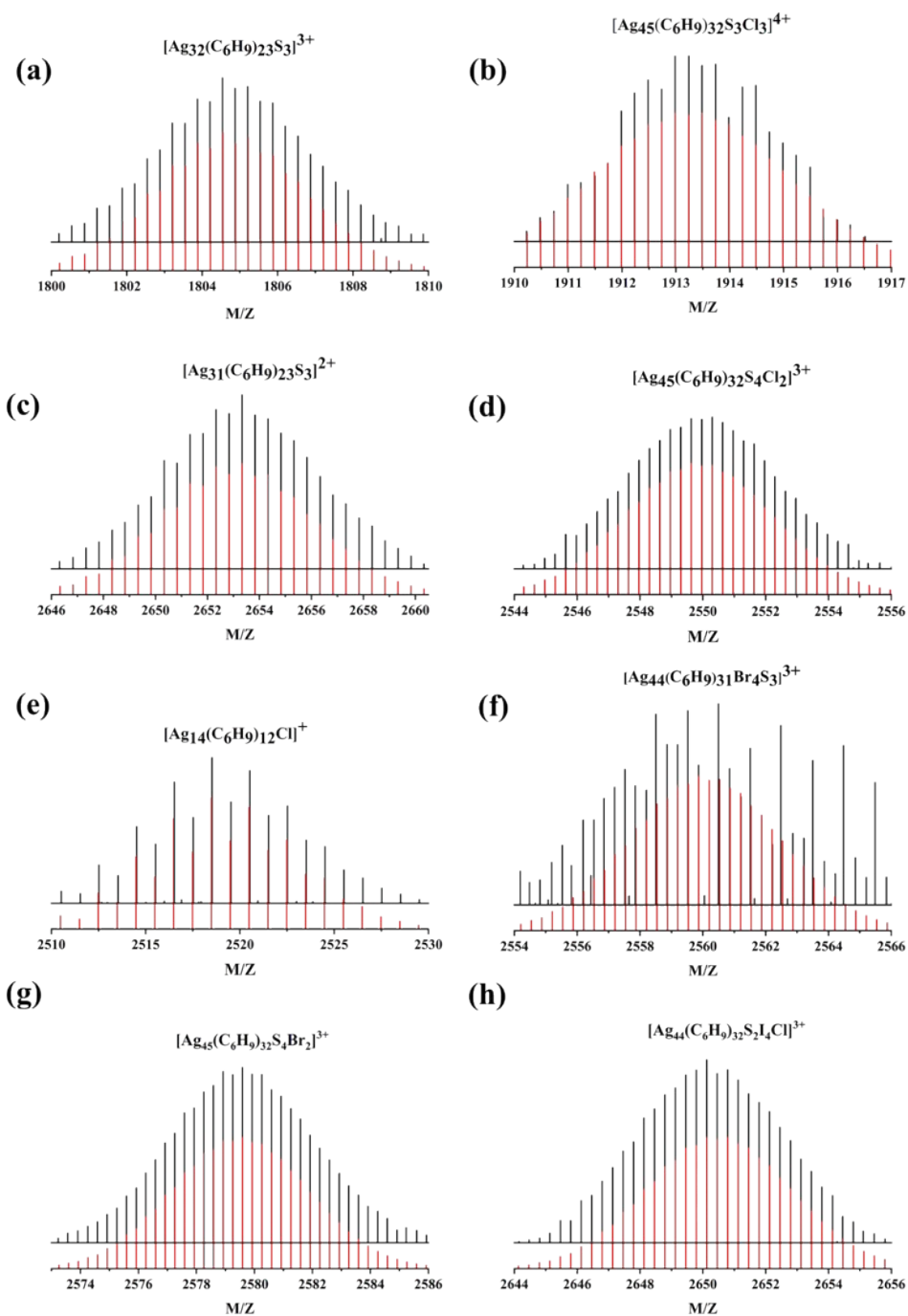


Figure S12. Comparison diagram of experimental peak (black line) and simulated isotope distribution peak (red line) within 1700-2700 M/Z.

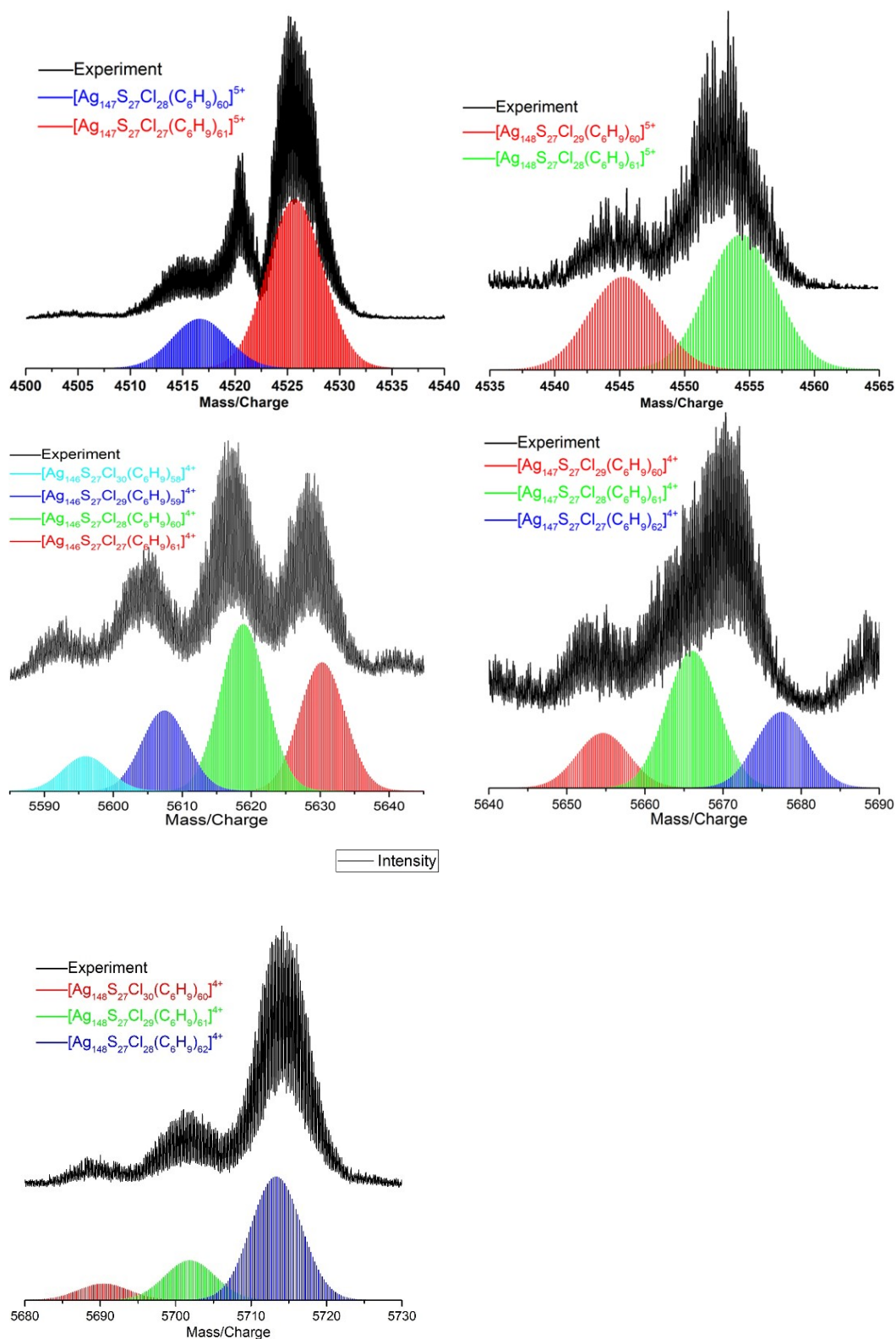


Figure S13. Fragments identified in ESI-MS of $\{Ag_{148}(ClIS)_{56}\}$.

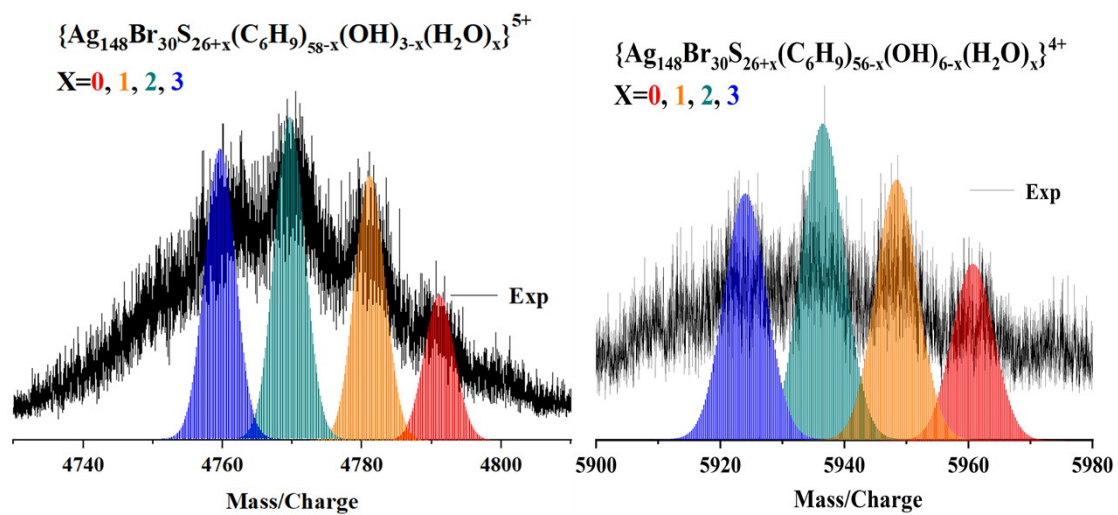


Figure S14. Fragments identified in ESI-MS of $\{\text{Ag}_{148}(\text{BrS})_{56}\}$.